# Breast MRI Multi- Sequence Segmentation and Registration

João F. Teixeira[1,2]
jpfteixeira.eng@gmail.com

Sílvia Bessa[2]
silvia.n.bessa@inesctec.pt

Hélder P. Oliveira[2,3]
helder.p.oliveira@inesctec.pt

[1]Faculdade de Engenharia
Universidade do Porto, Porto, Portugal

[2]INESC-TEC
Porto, Portugal

[3]Faculdade de Ciências
Universidade do Porto, Porto, Portugal

## Abstract

Different sequences of the same medical exam, as for instance MRI's *T1w* and *Dyn*, display different image features that enable the segmentation of specific objects to be easier in one over the other. In breast cancer research, *T1w* addresses better the diverse breast anatomy, while *Dyn* outshines over lesion segmentation. The present study proposes a methodology to tackle an unapproached task, in order to facilitate the volumetric alignment of data retrieved from *T1w* and *Dyn* sequences, leveraging breast surface segmentation and subsequent registration. The process seems to have promising results as average two-dimensional contour distances are at sub-voxel resolution and visual results seem well within range for the valid transference of other segmented or annotated structures.

## 1 Introduction

Magnetic Resonance Imaging (*MRI*) is often performed on breast cancer patients and allows 3D image reconstruction of the breast as it captures regular interval slices from the patient's torso. Image processing methods are often used to analyse these challenging *MRI* sequences, namely focusing on T1-weighted (*T1w*) and MRI Dynamic Contrast-Enhanced (MRI-DCE, *Dyn* henceforth). Specific objects in the torso are enhanced on particular sequences and so, it stands to reason focusing the development efforts towards dealing with the clearer options first.

The present study is an adaptation of [5], which aims to automatically obtain the breast anterior surface on *T1w* and on *Dyn* at instant zero (*Sd0*). Also, to join lesion annotations with the remaining anatomy reference points, the segmented surfaces from *T1w* and *Sd0* are registered using a simplification of the Iterative Closest Point algorithm (ICP).

### 1.1 Related Work

Across multiple cancer specificities, and breast cancer research in particular, there is a significant amount of data and methods associated with segmentation and multi-modal registration or fusion.

Segmentation approaches range from Maximum a Posteriori Estimation approaches, Expectation Maximization–Markov Random Field techniques and Atlas-based approaches to U-Net methodologies. However, research does not focus as much on *T1w* or *T2w* sequences as it does on *Dyn*, due to the lower difficulty of lesion segmentation on that sequence. Furthermore, those segmentation procedures are largely directed only towards the lesion and generally customarily the breast surface.

Breast multi-modal registration tasks generally involve fusing the *Dyn* sequences to other entirely different modalities, such as PET and CT [1], or between the 3D three-dimensional (3D) MRI and 2D data such as X-ray Mammography [3]. There are also human biology based works that focus on intra-modality alignment, commonly associated with the monitoring of some disease's progression, as usually found applied to brain CT scans [4]. Nevertheless, some similar work is also done with breast *Dyn* sequences [2].

However, this paper seems to be among the earlier work concerning *MRI* intra-patient registration between *T1w* and *Dyn* or derived subsequences, as in *Sd0*. Hence, we start studying low complexity approaches such as edge detection, contour refinement and rigid registration.

## 2 Dataset

The dataset used was provided by the *Redacted* project and consists of *T1-weighted* thoracic MRI exams (*T1w*) from 27 breast cancer patients, obtained with a Philips Ingenia 3.0T MRI scanner. Each exam comprises 60 gray-scale axial images, with the approximate dimensions of 3 mm thickness and resolution of $720 \times 720$ pixels (0.3-0.5 mm/pixel). Additionally, each *T1w* acquisition has a corresponding dynamic contrast study (*Dyn*) that includes the sequence data at the instant zero (*Sd0*). In turn, this sequence comprises 300 gray-scale sagittal images, with 1 mm thickness and a resolution of $300 \times 300$ pixels (0.5-0.6 mm/pixel), in a narrower field of view.

Due to the specific ease of annotating, the *T1w* also has available binary masks for the breast and the *Sd0* has the lesion we aim to transport (Figure 1). All annotations were manually performed by experts with more than 5 years of experience.

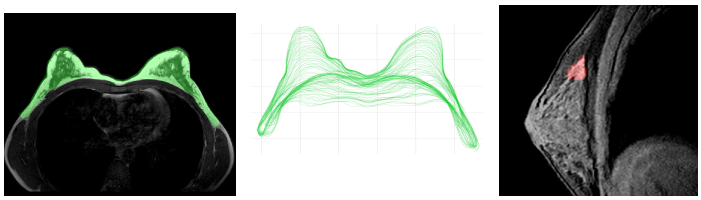

(a) *T1w* breast (b) *T1w* breast perimeter (c) *Sd0* Lesion

Figure 1: Annotation Images

## 3 Methodology

The tasks intended to be tackled include *T1w* and *Sd0* sequences' segmentation and subsequent registration of both segmented breast surfaces. For the segmentation task, *T1w* and *Sd0* volumes are individually processed using the same pipeline, despite their difference in field of view, voxel resolution and extent. *Sd0* volumes are rotated in 90 degrees, so that both anatomical volumes face the same direction, on the axial view.

### 3.1 Breast Surface Segmentation

The approach tries to enclose the breast surface in a solid region, ignoring internal structures when possible, enabling a smooth generation of the breast surface. The segmentation pipeline is shown in Figure 2.

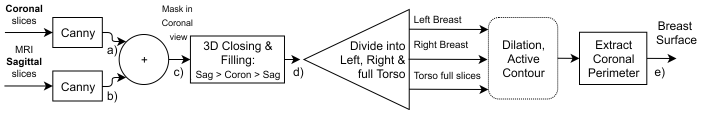


Figure 2: Segmentation Pipeline for one MRI sequence

The initial step is a Canny detector for obtaining the salient volume boundaries. This is performed in both coronal and sagittal directions (Figures 3a, 3b), to compensate potential gaps in perspective, namely hidden information of the inframammary folds. The edge maps are joined (Figure 3c) and closed with a 3D sphere. Flood-filling operations ensue: along the sagittal perspective, then along the coronal and again along the sagittal view (Figure 3d). Next we applied dilation filtering and a Chan-Vese level-set block, over the coronal view. This processing is done individually on separated left and right breast images, until a single object is found on the filling step. This avoids fusing the breasts on the active contour step. Lastly, the surface perimeter is then extracted (Figure 3e). An example of the 3D segmentation extents for a full patient is shown in Figure 4.

### 3.2 Registration

First we convert the coordinates of the point clouds to real world values (voxel resolution is applied to the point list). A point cloud is rotated

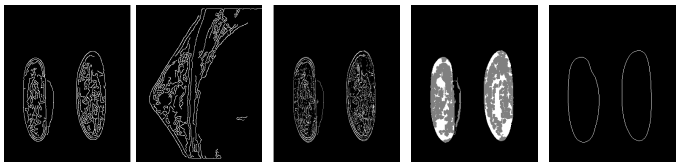

(a) Canny Coronal (b) Canny Sagittal (c) Mask Coronal (d) Filling (e) 3D Coronal Perimeter

Figure 3: Pipeline intermediate results for *Sd0*

so both (*Sd0* and *T1w*) face the same orientation. The point clouds are subsequently processed by an ICP algorithm, that imposes a no rotation restriction, as both sequences of data are captured during the same session and with the patient lying down, trying not to move. This will enable to accurately convert the desired spatial data - in this case the lesion's points acquired on the *Sd0* - and place it on the respective location, among the structure data on the base view (here, the *T1w*). An example of the process is shown in Figure 5.

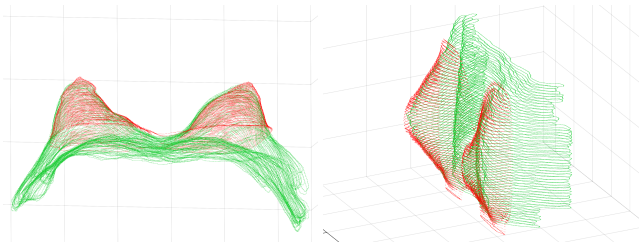

Figure 4: *T1w* Segmentation output (red) against GT contour (green)

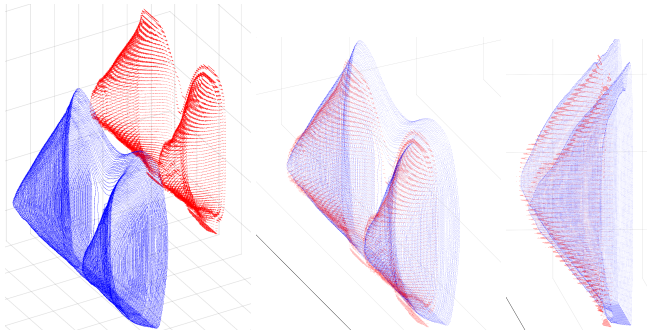

(a) Pre-Registred (b) Registred (c) Registred

Figure 5: Registration step. *T1w* (red), Registered *Sd0* (blue)

### 3.3 Evaluation metrics

For segmentation we can only fairly compare the *T1w* segmentation with the *T1wGT*, as there is no breast GT mask for *Sd0*. Furthermore, it should only be done in one direction, as *T1wGT*'s perimeter also includes the posterior breast contour (Fig 1b). Registration wise, the metric is obtained only from the aligned surfaces as using the *T1wGT* contour could negatively impact the registration process due to its extensive perimeter.

In neither case, area metrics can be provided as the segmented frontal breast surfaces are not comparable to the solid *T1wGT* objects. Hence, the metrics performed are *Average Distance* (one way) and *AD* (bidirectional). Extreme valued cases across all patients are also shown.

## 4 Results and Discussion

First, we observed an increasing surface distance as we reached the vertical extremities (Figure 4). It was expected as less homogeneous intensities are found in the top and bottom slices. In turn, this influences the segmentation method which operates on the sagittal and coronal perspectives and slightly expands the real boundaries to obtain a smoother, closed result.

The registration process of the segmented surfaces (Figure 5) presents acceptable alignments, where larger mismatches may be attributable to segmentation errors at the vertical extremities, in particular of the *T1w* surface. The breast shape acquired from both sequences seems to match enough to conduct reliable registration, producing an average error around the central slices of approximately the 4mm.

When comparing to *T1wGT*, the *Sd0* follows closely the outer skin interface, while the *T1w* segmentation follows the inner one, in many cases having the manual annotation averaging between both.

Table 1 presents numerical evidence of the results. The 3D *T1w* segmentation results point to about a 4 to 7 pixel error, which is a good result, considering some of the method's limitations and the reliability of the dataset.

Table 1: Segmentation and registration 3D errors

| | **Min** | **Avg. Dist.** | **AD** | **Max** |
|---|---|---|---|---|
| *T1w* to *T1wGT* | 1.23 | 2.20 (0.47) | *n.a.* | 3.05 |
| *Sd0* to *T1w* | 1.75 | 2.91(1.30) | 2.57 (1.01) | 6.17 |
| *T1w* to *Sd0* | 1.37 | 1.77 (0.47) | | 3.76 |

All metrics in mm (min is best). Avg. Dist. and AD present values averaged across all patients, and respective standard deviations in parenthesis.

On the registration side, a trend of larger *Sd0* to *T1w* error was anticipated and verified, as the *Sd0* has roughly 3 times more slices than *T1w*, for the same vertical extent. General errors are quite low considering that *T1w* has a slice thickness of 3 mm. The Avg. Dist. values are close, confirming that both segmentation surfaces have fairly similar shapes and extents. This validates the balanced method performance across both sequences. This also argues for the capacity of this ICP setup for the intended objective. Finally, and naturally, AD middles the Average Distance of each sequence, leaning more on the *Sd0* to *T1w* direction, as *Sd0* tends to have more points on the clouds than *T1w*.

## 5 Conclusion

An early pipeline for the untried fusion between the breast outer contour of *T1w* and *Sd0 MRI* sequences has been proposed. The main objective was to unify both sequences under the same orientation and 3D space, to combine both sources of annotations.

For this, a breast surface segmentation plus registration approach was employed. Both visual and quantitative outcomes show encouraging results, managing average contour distances below *T1w*'s slice thickness value. Although the approach may require further adjustments for an atlas development and other goals, the proposed pipeline seems to fulfill the purpose of joining the annotations of these two sequences.

**Acknowledgements:** This work is financed by National Funds through the Portuguese funding agency, FCT - Fundação para a Ciência e a Tecnologia within project UIDB/50014/2020, and PhD grants number SFRH/BD/135834/2018 and SFRH/BD/115616/2016.

## References

[1] I.D. Dmitriev, C.E. Loo, W.V. Vogel, K.E. Pengel, and K.G.A. Gilhuijs. Fully automated deformable registration of breast DCE-MRI and PET/CT. *Phys. Med. Biol.*, 58(4):1221–1233, 2013.

[2] Y.C. Gong and M. Brady. Texture-Based Simultaneous Registration and Segmentation of Breast DCE-MRI. In *Digital Mammography*, pages 174–180, 2008.

[3] T. Hopp, P. Baltzer, M. Dietzel, W.A. Kaiser, and N.V. Ruiter. 2D/3D image fusion of X-ray mammograms with breast MRI: visualizing dynamic contrast enhancement in mammograms. *J Comput Assist Radiol Surg*, 7(3):339–348, 2012.

[4] A. Klein, J. Andersson, B.A. Ardekani, J. Ashburner, B. Avants, M. Chiang, G.E. Christensen, D.L. Collins, J. Gee, P. Hellier, J.H. Song, M. Jenkinson, C. Lepage, D. Rueckert, P. Thompson, T. Vercauteren, R.P. Woods, J.J. Mann, and R.V. Parsey. Evaluation of 14 nonlinear deformation algorithms applied to human brain MRI registration. *Neuroimage*, 46(3):786 – 802, 2009.

[5] J.F. Teixeira, S. Bessa, P.F. Gouveia, and H.P. Oliveira. A Framework for Fusion of T1-Weighted and Dynamic MRI Sequences. In *Pattern Recognit. Image Anal.*, pages 157–169, 2020.